Remote Sensing Applications: Society and Environment 38 (2025) 101564

Contents lists available at ScienceDirect

Remote Sensing Applications: Society and Environment

journal homepage: www.elsevier.com/locate/rsase

Method for assessing volumetric solar potential within urban street canyons

Teresa Santos [a,*], Márcia Matias [b], Jorge Rocha [b,c,**], Killian Lobato [d,***]

[a] Interdisciplinary Centre of Social Sciences (CICS.NOVA), NOVA School of Social Sciences and Humanities (NOVA FCSH), Universidade NOVA de Lisboa, Av. de Berna, 26 C, 1069-061, Lisboa, Portugal
[b] Centre of Geographical Studies, Institute of Geography and Spatial Planning, University of Lisbon, 1600-276, Lisboa, Portugal
[c] Associate Laboratory Terra, Lisbon, Portugal
[d] Instituto Don Luiz, Faculdade de Ciências, Universidade de Lisboa, Lisboa, 1749-016, Portugal

A R T I C L E I N F O

Keywords:
Volumetric solar potential
Urban solar planning
City-scale solar analysis
GIS-Based solar analysis
Urban morphology and solar potential

A B S T R A C T

While rooftops have been extensively studied for their photovoltaic (PV) potential, the volumetric space between buildings remains largely unexplored. This study introduces a replicable framework to quantify solar radiation within this unoccupied urban volume. The methodology leverages widely available city-scale datasets (e.g., LIDAR data, elevation contours, and building footprints) and accessible software to generate virtual surfaces at incremental heights between buildings. These surfaces serve as the basis for calculating solar insolation at 30-min intervals. The approach is demonstrated using neighbourhoods with differing urban morphologies to showcase its applicability across various contexts. This framework produces detailed insolation maps, revealing how volumetric solar radiation varies with urban form and time of year. The use of city-scale datasets makes this approach particularly suited for planning at the urban scale, enabling urban planners to identify optimal locations for PV installations, enhance urban thermal comfort, and improve street luminosity. The primary contribution of this study lies in the accessibility and generalizability of the methodology, which can be applied to support urban design decisions where solar insolation is a critical factor. By addressing the underexplored volumetric solar potential, this study provides actionable tools for advancing urban sustainability.

1. Introduction

The 21st century has been referred to as "the century of urbanization" (Kanters et al., 2014). Future cities will face the need to optimize their energy demand significantly while shifting to local urban energy production. In the context of climate change, cities must adapt to the many challenges that these alterations may bring. Increased use of active solar energy as well as an awareness of the passive use of solar energy (by solar gains and daylight) is required in order to attain sustainable solutions (Kanters et al., 2014).

Cities have two-dimensional features, such as land use or land cover and the landscape, and three-dimensional features such as structures (buildings) and vegetation, that have changed significantly during the rapid urbanization process. These changes contribute

* Corresponding author.
** Corresponding author. Centre of Geographical Studies, Institute of Geography and Spatial Planning, University of Lisbon, 1600-276, Lisboa, Portugal.
*** Corresponding author.
E-mail addresses: teresasantos@fcsh.unl.pt (T. Santos), jorge.rocha@campus.ul.pt (J. Rocha), klobato@fc.ul.pt (K. Lobato).

https://doi.org/10.1016/j.rsase.2025.101564
Received 24 July 2024; Received in revised form 14 April 2025; Accepted 18 April 2025
Available online 23 April 2025

to the increased absorption of solar energy, modify the solar energy that some urban areas receive at the bottom of urban canyons and contribute to urban atmosphere warming (Vujovic et al., 2021). The amount of received radiation is directly linked to the angle of obstruction (visible sky). The obstruction of the sky is caused by the height of the buildings, the width of the streets and the height and position of the Sun (Rodrigo, 2016).

The irradiance received for one surface can be measured by ground-based meteorological stations or meteorological satellites and/or estimated through models. Regarding the latter, there are several examples, such as the Area Solar Radiation tool (Fu and Rich, 1999) or the Photovoltaic Geographical Information System (PVGIS), developed by the European Commission and the National Renewable Energy Laboratory (NREL) of the USA (Psomopoulos et al., 2015).

Over the past several years new methods and tools have been introduced into urban planning, such as assessment methods aiding urban planners and property owners to estimate the solar energy potential of existing built surfaces (Akrofi and Okitasari, 2022; Kanters, 2015; Lobaccaro and Frontini, 2014). Solar technologies are now commonly applied in the urban environment, such as rooftops (Assouline et al., 2017; Tian et al., 2021). Typical applications include electricity (photovoltaic - PV) and water heating.

One can argue that open spaces between buildings, such as streets and squares, are returning to pedestrian and soft mobility modes (Yoshimura et al., 2022). As such, these spaces, where there are no buildings, have the potential for the implementation of new solar energy structures (Rodrigo, 2016). Insofar, existing studies have mainly focused on the solar potential of the top of buildings. Studies evaluating solar availability in open spaces have primarily focused on the impact of urban morphology on ground-level solar exposure (Zhang et al., 2012; van Esch et al., 2012; Mohajeri et al., 2016; Chatzipoulka et al., 2016; Erdélyi et al., 2014; Lobaccaro et al., 2017; Zhu et al., 2019; Singh et al., 2023). However, none of these studies have estimated the volumetric solar potential within street canyons. This study addresses the gap in existing research by exploring whether volumetric solar potential in urban street spaces can be effectively quantified using accessible and widely available tools and datasets. To the best of our knowledge, this is the first work to demonstrate this capability.

This work will report, in detail, a method (first described by Rodrigo (2016)) to model the volumetric solar potential of complex urban environments. Rodrigo (2016) used this method to analyse the solar potential for intelligent urban furniture and services. Previously, Santos et al. (2020), addressed the solar potential of common urban structures in the public space, such as bus shelters. The authors proposed a methodology where the solar energy exposure of a point at any height above the street level within the unoccupied volume of an urban environment could be easily modelled. By analysing specific points pertaining to the surface of bus stop shelters in the city of Lisbon, they concluded that 54 % of all current shelters had the potential to receive PV-based solutions. Mordomo (2018) also used this method to evaluate the viability of installing solar streetlights. In this case, the results obtained for a Lisbon neighbourhood comprised of medium sized buildings with a compact layout showed that 50 % of the existing streetlights could be powered by solar panels.

The application of solar panels to electric vehicles (Brito et al., 2021) to increase per-charge range or reduce operating costs may benefit from the identification and mapping of parking spots with high solar insolation. The same can be argued for urban irrigation systems, street lighting, illumination of public buildings and monuments, small street buildings such as kiosks and bus stops, information and advertising boards, and e-bike charging stations or bus charging stations.

Beyond conventional applications, it is essential to explore innovative ways solar energy can support diverse activities and contribute to urban development. Solar-accessible volumes within urban canyons may offer opportunities for supporting PV infrastructure, particularly in cases where rooftop systems are limited by shading or structural constraints. For example, in developing countries where people do not have reliable access to the electricity grid, publicly placed PV in urban areas could serve this population to provide basic electricity needs. Another use could be related to housing conditions in countries with severe temperatures in summer and in winter, using PV for the air conditioning or domestic space heating, which would not be possible with only rooftop PV of tall buildings.

In the context of climate change and increasing city sustainability there are several approaches for using and repurposing public spaces. Local concerns about climate change and the public health implications of widespread motorization tend to be the primary obstacles addressed (Zipori and Cohen, 2015). As urban mobility evolves, particularly with the rise of automated vehicles and shared transport systems, traditional street layouts may shift significantly. A reduction in car ownership and on-street parking could free up portions of streets currently occupied by stationary vehicles (González-González et al., 2020; Lee et al., 2022). This transition offers a unique opportunity to reconfigure these urban spaces — including for energy purposes — by integrating solar infrastructure in locations with high volumetric irradiance potential It is our opinion that the redesign of cities can take into account the use of open spaces to install solar energy infrastructures. Another study presents the "superblock model" as a potential solution for improving health outcomes in urban areas (Mueller et al., 2020). The superblock model involves redesigning city blocks to prioritize walking, cycling, and public transit, and limiting car traffic to perimeter streets. The authors argue that this model can reduce air and noise pollution, increase physical activity, and improve mental health. Again, it is our opinion, that with this street model, solar infrastructure can also be implemented in the public spaces because the street is no longer heavily dedicated to the car.

2. Methods

We start by describing the method of how the solar potential of the urban volume is modelled. We then demonstrate its application to three test areas with differing urban morphologies.

A series of virtual surfaces are generated at incremental heights above the ground level. As shown in Fig. 1, these surfaces are created by systematically increasing the height of the digital surface model, at defined intervals, while the geometry of buildings remains unchanged. This approach allows for the calculation of solar insolation at various heights within the unoccupied urban volume, providing a detailed understanding of how solar radiation varies with height and surrounding urban morphology. By generating and evaluating the solar insolation of these surfaces, the methodology quantifies solar potential across a three-dimensional intrabuilding urban volume.

To generate the virtual surfaces, the following methodology was applied, as illustrated in Fig. 2. First, a Digital Surface Map (DSM) of Lisbon, created from 1 × 1 m^2 LIDAR data,[1] was combined with a building location map[2] to identify buildings and their respective heights. This step produced a detailed map of building heights. However, LIDAR data was not used to determine street height due to the presence of obstructions such as trees, cars, and temporary structures. Instead, a Digital Terrain Model (DTM) was created from cartographic data. The DTM was generated by first constructing a Triangulated Irregular Network from elevation mass points and contours, which was then converted into a 1 × 1 m^2 grid representing ground-level elevations. Santos (2011) provides a detailed discussion of the DTM and DSM.

Using the DTM and the building height map, sequential DSMs were generated by incrementally increasing the ground height by 1-m intervals, while keeping the building heights unchanged. These virtual surfaces form the basis for the volumetric analysis of solar potential within the urban environment.

The Area Solar Radiation tool (part of the ArcGIS Pro Spatial Analyst Extension provided by ERSI and previously known as the Solar Analyst tool) was then run for all the newly generated DSMs. For the purpose of demonstration, two extreme days were chosen, which stand for the best- and the worst-case scenarios for solar availability, the summer and winter solstices, respectively. Insolation maps were calculated, at 30-min intervals, and then summed to obtain the daily insolation maps for each height above street level.

The Area Solar Radiation tool has several parameters that can be adjusted trading calculation time for precision. Some parameters are applicable for direct solar irradiance, while others are applicable for diffuse irradiance. Upon reviewing this trade-off, the decision was taken to apply the maximum value permitted by the tool for each parameter to maximize the calculation precision for direct solar irradiance, while the default parameters were found to be sufficient for the diffuse solar irradiance. The parameters defining the intensity of direct and diffuse irradiance were adjusted to ensure that daily insolation, for the respective days, was the same as that reported by the PVGIS for Lisbon (Santos et al., 2020). The diffuse radiation model applied was Uniform Sky. Any surface orientation could have been considered, as this is an input option of the Area Solar Radiation tool, however only horizontal insolation was considered.

The solar radiation values (expressed in Wh m^{-2}) calculated for each surface point at each elevation level correspond to the cumulative energy that would be received by a horizontal surface placed at that location over the simulation period. These values indicate the solar energy flux that would pass through that horizontal surface area.

The method was applied to three test areas in Lisbon with distinct urban morphologies (see Fig. 3). Lisbon is part of a metropolitan area with 2.8 million inhabitants. Located on the Atlantic coast of Portugal, the city has an average of 8 h of sunshine per day. Lisbon is characterized by a Mediterranean climate and a hilly topography.

Salgueiro describes how Lisbon has developed (Salgueiro, 2002) and argues that Lisbon Metropolitan Area has grown in an unplanned way. The city's development reflects the growth peaks in economic expansion periods and a lower growth rate in recessive periods. Lisbon is a heterogeneous city from the morphological point of view, where different types of designs reflect the ways and the time in which they were built.

Lisbon's morphologies can be seen as an attribute which defines solar potential. For that reason, the three chosen test areas present different urban morphologies, which in turn influence the insolation characteristics of the area.

The *Parque das Nações* (translates to Nation's Park) area is a modern, waterfront district, featuring futuristic architecture, wide, tree-lined boulevards, and ample public spaces, the result of urban redevelopment for Expo '98. The *Baixa de Lisboa* (downtown Lisbon) is characterised by its orthogonal, grid-like street pattern, neoclassical architecture, and grand plazas, a reflection of the 18th century Pombaline rebuilding following the 1755 earthquake. Finally, *Madredeus* (translate to mother-of-God) neighbourhood is a traditional residential neighbourhood, marked by narrow, winding streets and historic two-story houses.

For all three areas, the daily insolation was calculated for a series of heights above street level for the two distinct days. The results are, as a function of height, a series of solar insolation maps (calculated at 30-min intervals), which are then combined to form a daily insolation map. For the three areas of study, two streets in each area were selected for a detailed presentation of the generated insolation data.

Atlântico Avenue (PN1) and D. João II Avenue (PN2) were chosen for the study location of Parque das Nações. PN1 is 36 m wide and is orientated E/W. This avenue is almost 2.8 km long. Residential, commercial and hotel structures of all kinds are present here. PN2 street is N/S oriented and 60 m wide. This street is where you'll find an array of buildings, including retail stores, convention centres, and the Justice Campus (Campus da Justiça). The current structures in these streets are all approximately 30 m tall.

Augusta Street (BL1) and Comércio Street (BL2) were chosen in Baixa de Lisboa. One of Lisbon's most well-known areas, Baixa de Lisboa is frequently crowded with visitors, especially during the day, peaking during the summer. BL1 is 15 m wide and is N/S-oriented. There are some residences, small businesses, hotels, local shops, and restaurants on this street. BL2 is 14 m wide and has an E/W orientation. Buildings in BL2 generally fall into the same categories as BL1. Both BL1 and BL2 have neighbouring structures that are at least 30 m high.

The streets José Leilote (MD1) and Dom José de Bragança (MD2) were chosen for the Madre Deus study location. MD1 is 260 m long, 12 m wide, and is oriented NW/SE. There are primarily homes in this area. MD2 is NE/SW oriented and is 20 m wide. Identical to

[1] Data is freely available upon request to authors.
[2] Data is freely available at the Open Street Map website.

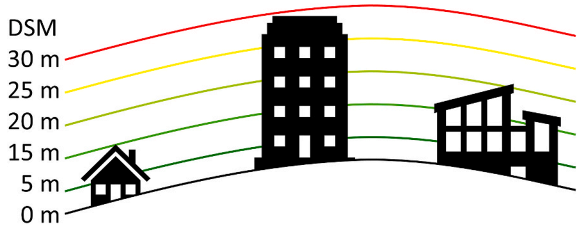

Fig. 1. Schematic representation of the methodology for generating virtual surfaces.

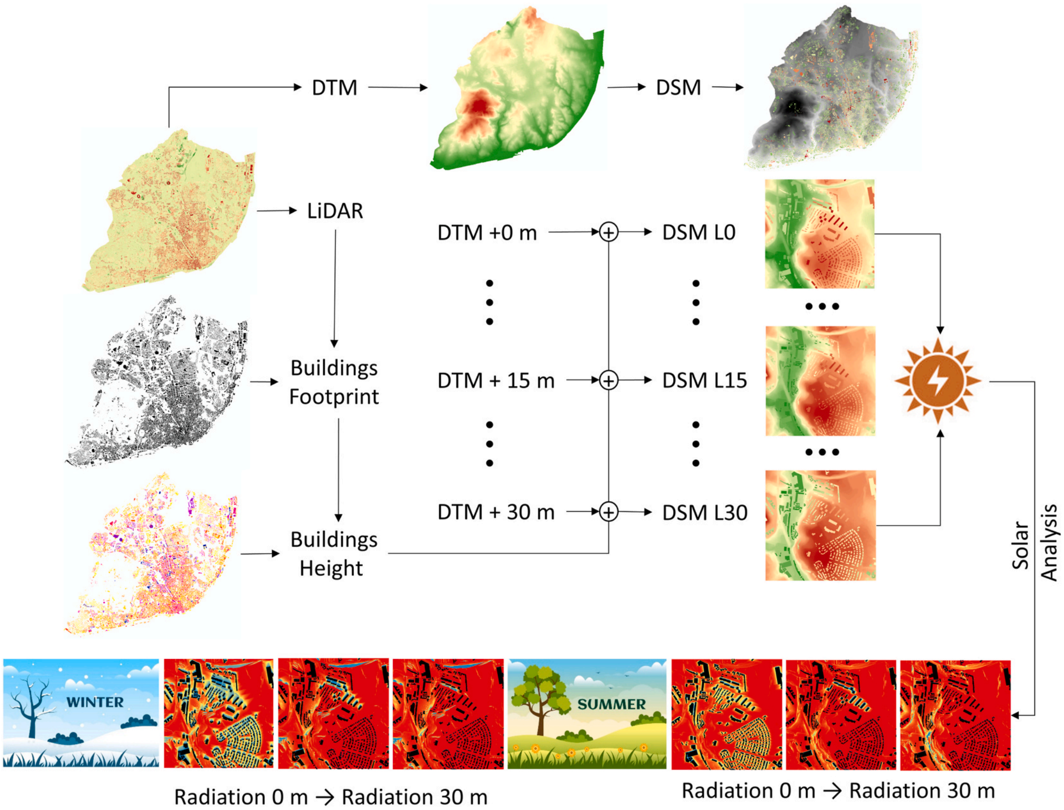

Fig. 2. Schematic representation of the generation of Digital Surface Maps required for the subsequent daily insolation maps calculated for different heights above the street level.

the MD1 street, each building on this street is a residence. At 7 m in height, the buildings in these two streets are the lowest of the three locations under consideration.

3. Results

All results shown are cross-sections of the calculated daily insolation maps. The daily insolation maps can be consulted in the supplementary materials.

Fig. 4 represents the output of the processed data, in cross-section, for the daily insolation of two streets in Baixa de Lisboa (BL), for summer and winter solstices. These types of figures can be generated for any section of the streets for the studied areas. The chosen streets are similar in terms of width and surrounding buildings' height. However, the two streets have differing orientations, BL1 with an almost direct N/S orientation, whilst BL2 has an almost direct E/W orientation. The horizontal resolution was 1 m, limited by LIDAR data. The vertical resolution was set at 1 m height increments and deemed sufficient for presentation purposes. To aid visual clarity, pedestrians, vehicles, and solar-powered streetlights are depicted. The red coloured zones are areas where there is essentially no shading from buildings. The grey colouring represents the buildings. For the two streets, the skyview maps with the solar path, from the centre of the street are shown for three selected heights above street level.

In the summer solstice, for the street with a mainly N/S orientation (BL1), we can see that most of the volume of the street has a high

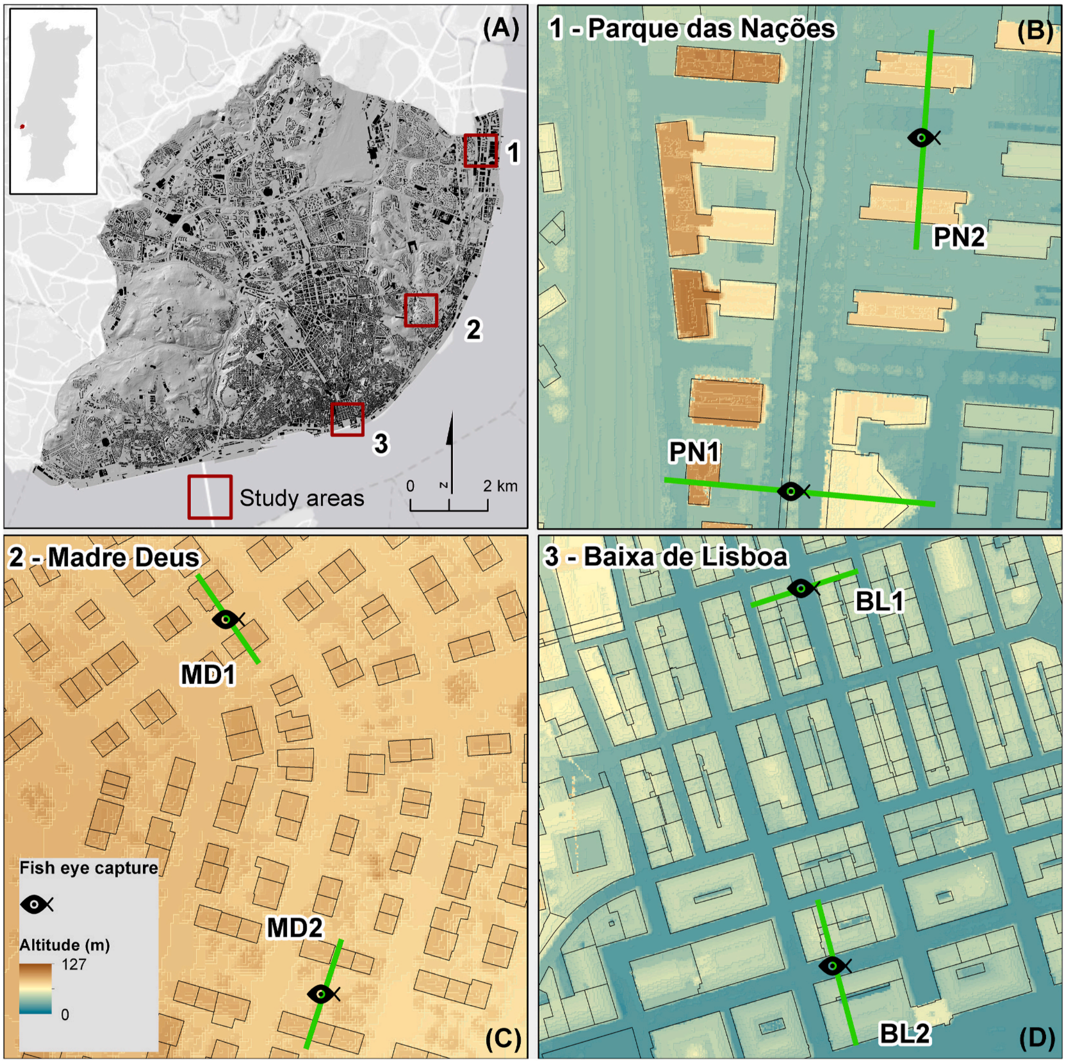

Fig. 3. A) The municipality of Lisbon. The red square denotes the neighbourhood areas selected for the study. Elevation maps of the study areas: b) Parque das Nações (PN); c) Baixa de Lisboa (BL); and d) Madre Deus (MD). The green lines with the fish-eye icons indicate specific street cross-sections (PN1, PN2, BL1, BL2, MD1, and MD2) where results presented later in the manuscript were analysed. Altitude scale denotes height of identified buildings.

and uniform level of insolation. However, because the street has a slight NW/SE direction, the western side of the street will receive less sunlight than the eastern side of the street. This difference becomes less pronounced as the height increases. For the mainly E/W orientated street (BL2), there is a marked transition of the solar insolation at around 15 m. The south side of the street, as expected for Lisbon's latitude, has a lower degree of insolation.

Regarding the winter solstice, for BL1 (N/S) there is a very sharp transition midway up the height. This transition starts at a lower height on the east side of the street (around 16 m) and higher on the west side of the street (around 23 m). The reasons for this are, again, the street is not perfectly aligned along the N/S direction. Regarding street BL2 with an E/W orientation, the volume of the street with a high degree of insolation is greater and the transition between high to low insolation volumes is less abrupt. In this case, the asymmetry between the south and north sides of the street is not only due to not being perfectly aligned with the E/W orientation, but it is because there are taller buildings on the west side of the street when compared to the east side (see skyview maps at 20 m).

The sky-view maps with the solar paths superimpose help to clarify why with increasing height, for differing streets, one observes different solar insolation levels. The form of the horizons is similar as we move from street level to 10 and 20 m above street level. However, one is rotated with the respect to the other because of the respective street orientations. One can observe that the height is increased, there is a greater solar path which is now unobstructed, which correlates with the increased solar insolation at the respective height. One can also understand why the N/S orientated street has a greater solar insolation throughout the volume of the street when compared to the E/W oriented street.

In general terms, Fig. 4 shows that for narrow streets with tall buildings (a large height-to-width ratio), there is a substantial volume

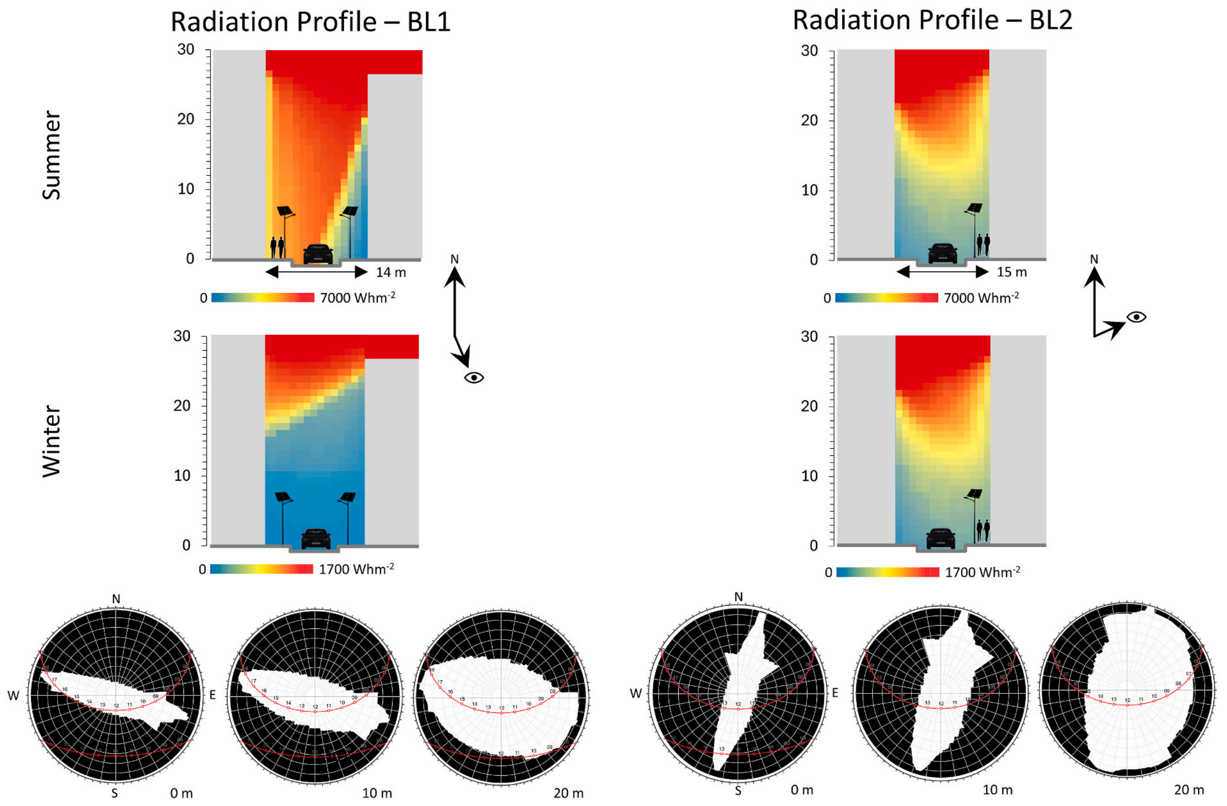

Fig. 4. Section views of the summer and winter solstice daily insolation (global horizontal) for the downtown area of Lisbon known as Baixa de Lisboa (BL) for two streets. BL1 has a strong N/S orientation. The figure views the street in the southerly direction, thus the left side of the figure corresponds to the east side of the street and the right side to the west side of the street. BL2 has a strong E/W orientation. The street is viewed in an easterly direction thus the left side of the figure corresponds to the northern) side of the street, and the right side corresponds to the southern side of the street. Also shown are the respective skyview maps at three heights. Note that the absolute daily insolation levels are significantly different between winter and summer. Solar radiation values (Wh m^{-2}) represent the cumulative energy that would be received by a hypothetical horizontal surface area placed at each elevation.

of the street which receives significantly less sunlight. However, streets with an E/W orientation have a significantly greater volume of the street with more solar insolation on the worst days of the year when compared to N/S-orientated streets. In essence, an E/W orientated street has a higher fraction of volume which is useable all year round.

Fig. 5 shows the same output of the daily winter and summer solstice insolation levels of two streets with tall buildings but with significantly wider streets when compared to the previous example (Baixa de Lisboa, Fig. 4). However, the street widths are not equal, PN1 has a street width of 36 m whilst PN2's is 60 m. PN1 is E/W orientated whilst PN2 is N/S orientated.

For the E/W-oriented street (PN1), the insolation patterns are similar to those previously shown for an E/W-orientated narrow street (see Fig. 4, BL2). The pattern is, however, more symmetric due to a combination of the street being more closely aligned with the E/W orientation and the skyview maps being more symmetric too. For the N/S orientated street (PN2) the insolation pattern is very different to the E/W street (PN1). However, it has similarities with the likewise orientated (N/S) but narrow street shown in Fig. 4 (PL1). Because the street is wider, a significant volume of the street has maximum insolation levels. Only a small fraction of the volume on the south side of the street has very low insolation levels. This is due to there still being buildings covering part of the horizon and solar path (see skyview map at 20 m for PN2).

In summary, the E/W orientated streets have similar insolation patterns when comparing narrow and wide streets. Insolation levels are always low near ground level. However, for N/S-orientated streets, the width of the street plays a significant role, impacting the volume which has high insolation levels. Wider streets benefit significantly as there is a significantly higher fraction of the street volume with high insolation levels.

Fig. 6 shows the output, in cross-section, of the daily insolation of two streets in Madre Deus (MD) in summer and winter solstices. This urban area is characterised by low-lying detached or semidetached homes. Although with similar surrounding buildings (7 m in height) they differ slightly in width (12 m and 20 m, for MD1 and MD2, respectively). They also differ in orientation, MD1 has an NW/SE orientation, whilst MD2 has a NE/SW orientation. Although their orientations are different, they are mirrored. As such, the results are also mirrored. For the summer solstice, the results show that almost the whole volume of the street has maximum insolation levels. However, near the walls (less than 2 m away) insolation levels are about half the maximum value. Moving to the winter solstice, we again see the already observed pattern of a sharp transition for streets deviating from a direct N/S orientation. For MD1, the north-

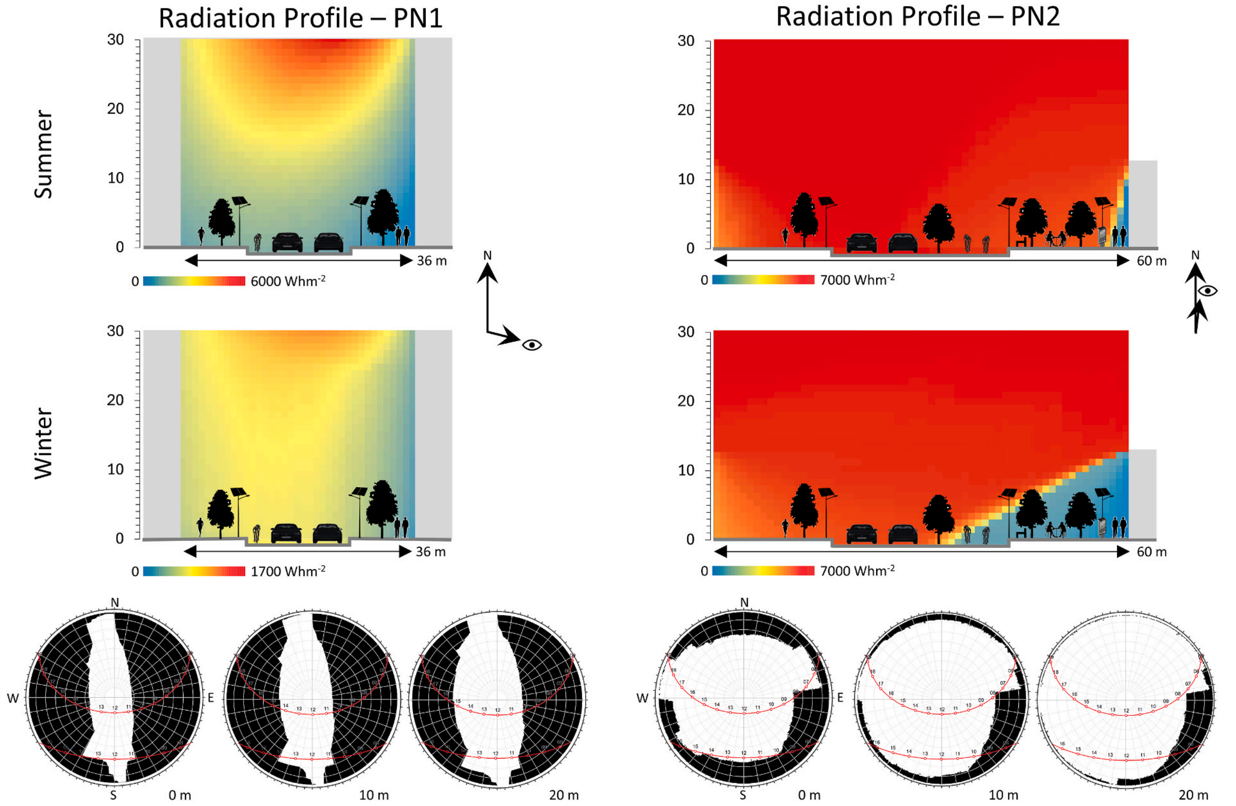

Fig. 5. Section views of the summer and winter solstice daily insolation (global horizontal) for the Parque das Nações area (PN) for two streets. PN1 has a strong E/W orientation. The figure views the street in an easterly direction, thus left side of the figure corresponds to the northern side of the street, and the right side corresponds to the south side of the street. PN2 has a strong N/S orientation. The figure views the street in the northerly direction, thus the left side of the figure corresponds to the east side of the street and the right side to the west side of the street. Also shown are the respective skyview maps at three heights. Note that the absolute daily insolation levels are significantly different between winter and summer. The vertical axis denoting height is the same in Fig. 4–6. However, the horizontal axis representing the street width has a different sale in all three figures. Solar radiation values (Wh m^{-2}) represent the cumulative energy that would be received by a hypothetical horizontal surface area placed at each elevation.

eastern side of the street is south facing and as such receives higher levels of insolation. The opposite occurs for MD2, where now it is the north-western side of the street which is SE facing and so receives higher levels of insolation. Due to the height-to-width ratio being close to 1 and the solar path at Lisbon's latitude exceeding 45° for only a few hours during the winter solstice, a considerable portion of the street receives minimal solar insolation.

4. Discussion

We have indicated in the introduction several examples where PV could be implemented in the volume above a street and between buildings. In areas with minimal shading (i.e., where the insolation level is very similar to that above building levels), the amount of PV required would not need adjustment. However, in volumes where the insolation level is 50 % of that found in unshaded areas, the installed PV power would need to double to achieve the same daily energy generation. For example, Santos et al. (2020) determined the PV potential of bus shelters. The methodology presented here could extend this context to identify which bus shelters could be modified to significantly increase their PV potential—whether by relocation or increasing their height.

Another application is identifying building façade heights with high solar insolation. Horizontal or vertical PV modules could be installed as façade extensions to collect solar radiation at optimal locations, while also providing shading to the building. For example, in a street with a predominantly E/W orientation and narrow spacing between buildings (see Fig. 3), PV modules placed below 10 m would have little or no productivity. Similarly, the vertical insolation can be calculated based on the façade's orientation relative to the Sun.

This methodology can also map the locations and heights in a street suitable for solar-powered streetlights. As shown in Fig. 5, during the winter solstice, one side of the street receives significantly less insolation, indicating the side more suitable for solar-powered streetlights. Additionally, the voxel data generated by this method can optimize the flight paths of solar-powered autonomous drones (UAVs) or vehicles, minimizing battery drain depending on the time of day and year.

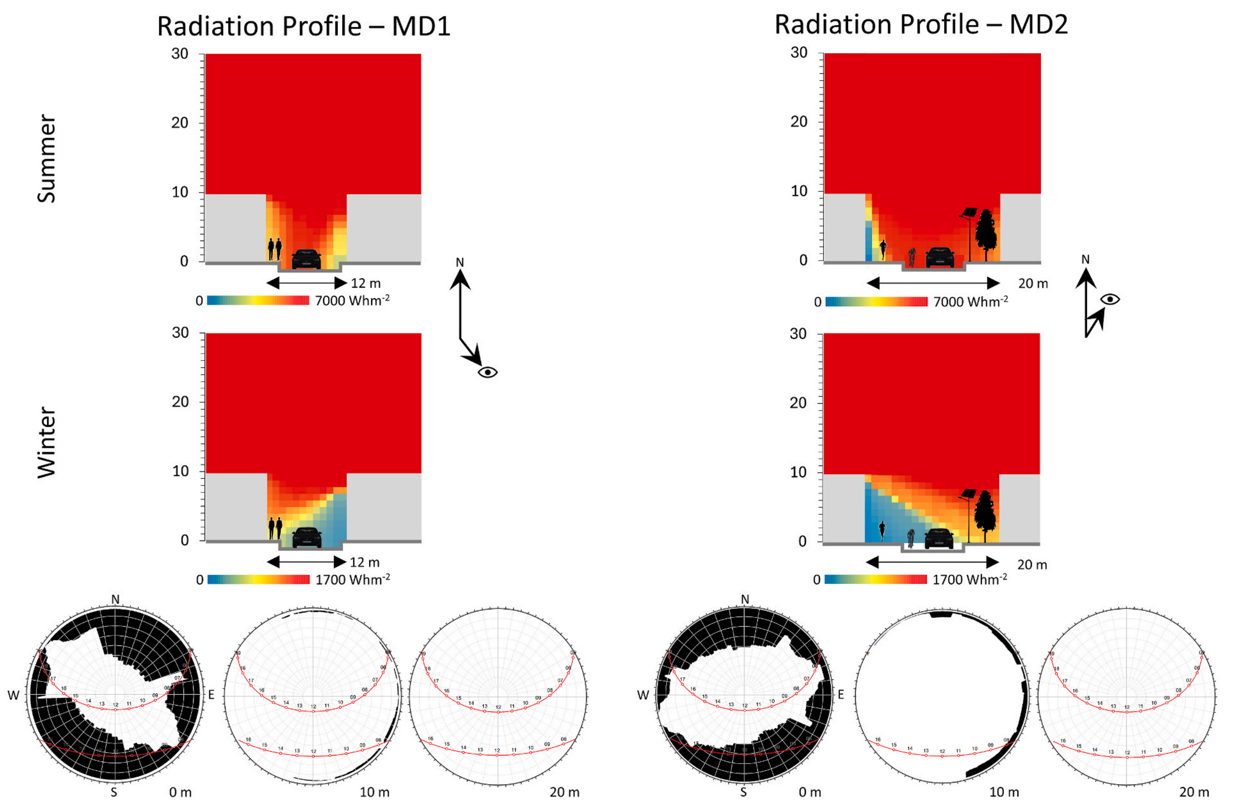

Fig. 6. Section views of the summer and winter solstice daily insolation (global horizontal) for the Madre Deus area (MD) for two streets. MD1 has an NW/SE orientation. The figure views the street in a south-easterly easterly direction, thus left side of the figure corresponds to the norther-eastern side of the street, and the right side corresponds to the south-western side of the street. PN2 has a NE/SW orientation. The figure views the street in the north-easterly direction, thus the left side of the figure corresponds to the north-western side of the street and the right side to the south-eastern side of the street. Also shown are the respective skyview maps at three heights. Note that the absolute daily insolation levels are significantly different between winter and summer. The vertical axis denoting height is the same in Fig. 4–6. However, the horizontal axis representing the street width has a different sale in all three figures. Solar radiation values (Wh m^{-2}) represent the cumulative energy that would be received by a hypothetical horizontal surface area placed at each elevation.

The data generated by this method can also support city-scale analyses of solar insolation, helping inform future policies regarding building efficiency codes. For instance, structures in high-insolation street locations, such as kiosks, public transport shelters, e-bike solar-powered shelters, or solar street lighting, could be mandated to include built-in PV. Similarly, sections of buildings with high-insolation façades could be treated differently from those building sections with low-insolation façades. Parking spaces for EVs with integrated PV could be mapped to ensure optimal charging conditions.

Solar cadastres (Giorio et al., 2025) and solar envelopes (De Luca and Dogan, 2019; Knowles, 2003) represent two established approaches to integrating solar potential into urban planning. Cadastres map solar irradiance on existing surfaces based on the urban geometry extracted from DSM data, and are valuable for estimating the feasibility of solar installations on roofs and façades. Solar envelopes, in contrast, define volumetric boundaries for new development that preserve solar access to surrounding properties. In comparison, our method evaluates solar potential throughout the open urban volume, independent of the presence of built surfaces. This enables the identification of solar-rich airspace zones that are often overlooked in surface-constrained methods, and offers complementary insight for vertical urban design and energy planning strategies.

The presented methodology has its limitations. Levels of diffuse radiation are heavily influenced by urban morphology, and good prior knowledge of the meteorological conditions in the area of study is required to ensure that the contribution of diffuse light is properly accounted for (Mordomo, 2018). For example, diffuse radiation can significantly contribute to PV module power generation (Brito et al., 2021). This study only considered clear-sky atmospheric diffuse radiation, which is proportional to the sky-view factor.

While incorporating diffuse irradiation for various climatic conditions is feasible, it introduces complexities related to selecting and implementing suitable diffuse irradiance models, which vary in accuracy and applicability. Future work could explore integrating these models to better account for overcast, partially cloudy skies, or localized weather conditions, thereby enhancing the methodology's applicability across diverse climates.

Similarly, the methodology does not yet consider reflected irradiance from urban surfaces such as buildings, streets, or vegetation. Reflected irradiance includes both diffuse and specular components, which depend on material properties and surface geometry. Accurately modelling reflectance would require detailed city-scale data on the angular and spectral dependencies of surface reflectivity. While a first-order approximation using Lambertian (diffuse) reflection is commonly applied in urban solar modelling, this approach still requires knowledge of surrounding material albedos and visibility between surfaces. Our method does not currently incorporate reflected irradiance due to limitations in the software used. Notably, tools such as the SEBE plugin (Lindberg et al., 2015) can incorporate ground-reflected radiation using a diffuse reflection model, but do not model façade-to-façade reflections. While ray tracing–based tools (e.g., Daysim, Radiance) and radiosity-based models (e.g., CitySim, SOLENE, R-CadSol) can simulate these interactions more fully, their computational demands or data requirements often limit their applicability at scale (Blaise and Gilles, 2022). We therefore acknowledge this as a limitation of our approach, especially in dense urban configurations where reflected radiation from façades can contribute significantly to total irradiance that would be incident on our hypothetical horizontal surface area. Furthermore, while the incremental elevation of the analysis surface affects the local sky view factor, this is correctly accounted for in the calculation of diffuse irradiance from the sky. However, if reflected irradiance were to be included, this artificial modification of the surrounding geometry would alter the visibility of reflective surfaces and result in non-representative estimates. We therefore limit our analysis to direct and diffuse sky components, acknowledging this as a constraint of the current implementation.

The methodology was demonstrated using seasonal extremes (summer and winter solstices), representing best- and worst-case scenarios for solar availability. However, the method can be applied to any solar declination to obtain representative data for any time of year, allowing for time-specific or period-summed analyses.

Additionally, the need for real-world validation of the methodology is acknowledged. This involves recording insolation levels at various heights and locations under diverse conditions, including shaded and open areas, different surface types, and multiple seasons. Incorporating these real-world measurements will ensure the robustness and reliability of the results for practical applications.

5. Conclusions

In this study, we introduced a straightforward and replicable methodology for assessing insolation levels in the volumetric open spaces between buildings in urban environments. Utilizing widely available tools, such as ArcGIS Pro with the Area Solar Radiation extension, and high-resolution digital surface maps, we generated virtual surfaces at varying heights above street level to calculate insolation levels. This approach enables the quantitative determination of solar potential at any point within the unoccupied urban volume. To demonstrate the method, we analysed three urban areas with distinct morphologies, revealing both similarities and differences in daily insolation patterns as a function of street orientation, local morphology, and time of year.

The methodology is accessible to individuals trained in GIS tools and does not require specialized computing hardware, making it practical for widespread adoption in urban planning. Its outputs offer a robust foundation for urban solar potential assessment, enabling planners to quantitatively identify volumes of interest. Beyond energy-related applications, the methodology can be applied at a city scale to map areas with high and low solar insolation. These insights allow the creation of metrics that quantify a city's performance in terms of solar access and related challenges.

Future research can further explore practical applications, such as optimizing the placement of PV systems (e.g., solar-powered streetlights, e-bike charging stations, or urban furniture) and designing shading strategies to enhance thermal comfort in pedestrian zones. However, future work should also include the study of different climatic regions with higher diffuse irradiance, the incorporation of urban surface reflection effects, and the experimental validation of the modelled insolation levels to ensure broader applicability and accuracy.

CRediT authorship contribution statement

Teresa Santos: Writing – review & editing, Writing – original draft, Visualization, Validation, Supervision, Software, Resources, Project administration, Methodology, Investigation, Funding acquisition, Formal analysis, Data curation. **Márcia Matias:** Writing – review & editing, Funding acquisition. **Jorge Rocha:** Writing – review & editing, Visualization, Validation, Supervision, Software, Resources, Investigation, Funding acquisition, Formal analysis, Data curation. **Killian Lobato:** Writing – review & editing, Validation, Supervision, Methodology, Funding acquisition, Formal analysis, Conceptualization.

EthicStatement

All authors confirm that the ethical guidelines stated in Elsevier's Publishing Ethics Policy were followed.

Declaration of generative AI and AI-assisted technologies in the writing process

During the preparation of this work the authors used OpenAI's ChatGPT (January 2024), to refine the language and grammar of the manuscript. After using this tool, the authors reviewed and edited the content as needed and take full responsibility for the content of the publication.

Funding

The first author acknowledges financing by the Fundação para a Ciência e a Tecnologia (FCT), under the Norma Transitória-DL 57/2016/CP1453/CT0004 and also by the Fundação para a Ciência e a Tecnologia (FCT) I.P./MCTES with the following grant number (PIDDAC) UIDB/04647/2020. The second author acknowledges financing by the Fundação para a Ciência e a Technologia (FCT) under the following PhD grant 2021.05248.BD. The third author acknowledges financing from Centre of Geographical Studies, University of Lisbon and FCT under Grant [number UIDB/00295/2020 + UIDP/00295/2020]. The fourth author acknowledges financing by the Fundação para a Ciência e a Tecnologia (FCT) I.P./MCTES with the following grant number (PIDDAC) UIDB/50019/2020.

Declaration of competing interest

The authors declare that they have no known competing financial interests or personal relationships that could have appeared to influence the work reported in this paper.

Appendix A. Supplementary data

Supplementary data to this article can be found online at https://doi.org/10.1016/j.rsase.2025.101564.

Data availability

Data will be made available on request.

References

Akrofi, M.M., Okitasari, M., 2022. Integrating solar energy considerations into urban planning for low carbon cities: a systematic review of the state-of-the-art, Urban Gov. https://doi.org/10.1016/j.ugj.2022.04.002.
Assouline, D., Mohajeri, N., Scartezzini, J.L., 2017. Quantifying rooftop photovoltaic solar energy potential: a machine learning approach. Sol. Energy 141, 278–296. https://doi.org/10.1016/j.solener.2016.11.045.
Blaise, R., Gilles, D., 2022. Adapted strategy for large-scale assessment of solar potential on facades in urban areas focusing on the reflection component. Solar Energy Advances 2, 100030. https://doi.org/10.1016/j.seja.2022.100030.
Brito, M.C., Santos, T., Moura, F., Pera, D., Rocha, J., 2021. Urban solar potential for vehicle integrated photovoltaics. Transport. Res. Transport Environ. 94, 102810. https://doi.org/10.1016/j.trd.2021.102810.
Chatzipoulka, C., Compagnon, R., Nikolopoulou, M., 2016. Urban geometry and solar availability on façades and ground of real urban forms: using London as a case study. Sol. Energy 138, 53–66. https://doi.org/10.1016/j.solener.2016.09.005.
De Luca, F., Dogan, T., 2019. A novel solar envelope method based on solar ordinances for urban planning. Build. Simulat. 12 (5), 817–834. https://doi.org/10.1007/s12273-019-0561-1.
Erdélyi, R., Wang, Y., Guo, W., Hanna, E., Colantuono, G., 2014. Three-dimensional SOlar RAdiation Model (SORAM) and its application to 3-D urban planning. Sol. Energy 101, 63–73. https://doi.org/10.1016/j.solener.2013.12.023.
Fu, P., Rich, P.M., 1999. Design and implementation of the solar Analyst: an ArcView extension for modeling solar radiation at landscape scales. In: 19th Annu. ESRI User Conf., pp. 1–24.
Giorio, M., Manni, M., Köker, N.I., Bertolin, C., Thebault, M., Lobaccaro, G., 2025. Interactive platforms for solar energy planning in smart cities: a state-of-the-art review of solar cadasters. Sol. Energy 287, 113227. https://doi.org/10.1016/j.solener.2024.113227.
González-González, E., Nogués, S., Stead, D., 2020. Parking futures: preparing European cities for the advent of automated vehicles. Land Use Policy 91, 104010. https://doi.org/10.1016/j.landusepol.2019.05.029.
Kanters, J., 2015. Planning for solar buildings in urban environments. An Analysis of the Design Process, Methods and Tools. Lund University.
Kanters, J., Wall, M., Dubois, M.C., 2014. Typical values for active solar energy in urban planning. Energy Proc. 48, 1607–1616. https://doi.org/10.1016/j.egypro.2014.02.181.
Knowles, R.L., 2003. The solar envelope: its meaning for energy and buildings. Energy Build. 35 (1), 15–25. https://doi.org/10.1016/S0378-7788(02)00076-2.
Lee, S., Jang, K.M., Kang, N., Kim, J., Oh, M., Kim, Y., 2022. Redesigning urban elements and structures considering autonomous vehicles: preparing design strategies for wide implementation in cities. Cities 123, 103595. https://doi.org/10.1016/j.cities.2022.103595.
Lindberg, F., Jonsson, P., Honjo, T., Wästberg, D., 2015. Solar energy on building envelopes – 3D modelling in a 2D environment. Sol. Energy 115, 369–378. https://doi.org/10.1016/j.solener.2015.03.001.
Lobaccaro, G., Frontini, F., 2014. Solar energy in urban environment: how urban densification affects existing buildings. Energy Proc. 48, 1559–1569. https://doi.org/10.1016/j.egypro.2014.02.176.
Lobaccaro, G., Carlucci, S., Croce, S., Paparella, R., Finocchiaro, L., 2017. Boosting solar accessibility and potential of urban districts in the Nordic climate: a case study in Trondheim. Sol. Energy 149, 347–369. https://doi.org/10.1016/j.solener.2017.04.015.
Mohajeri, N., Upadhyay, G., Gudmundsson, A., Assouline, D., Kämpf, J., Scartezzini, J.-L., 2016. Effects of urban compactness on solar energy potential. Renew. Energy 93, 469–482. https://doi.org/10.1016/j.renene.2016.02.053.
Mordomo, C.F., 2018. Potential PV No Espaço Público Urbano. Universidade de Lisboa. http://repositorio.ul.pt/handle/10451/36393.
Mueller, N., Rojas-Rueda, D., Khreis, H., Cirach, M., Andrés, D., Ballester, J., Bartoll, X., Daher, C., Deluca, A., Echave, C., Milà, C., Márquez, S., Palou, J., Pérez, K., Tonne, C., Stevenson, M., Rueda, S., Nieuwenhuijsen, M., 2020. Changing the urban design of cities for health: the superblock model. Environ. Int. 134, 105132. https://doi.org/10.1016/j.envint.2019.105132.
Psomopoulos, C.S., Ioannidis, G.C., Kaminaris, S.D., Mardikis, K.D., Katsikas, N.G., 2015. A comparative evaluation of photovoltaic electricity production assessment software (PVGIS, PVWatts and RETScreen). Environ. Process. 2, S175–S189. https://doi.org/10.1007/s40710-015-0092-4.
Rodrigo, C.M., 2016. Potential Solar Em Espaço Livre Urbano. Universidade de Lisboa. https://repositorio.ul.pt/handle/10451/26016.
Salgueiro, T.B., 2002. Desenvolvimento Urbano de Lisboa. Rev. Estud. Reg. 7–22.
Santos, T., 2011. A Methodology to Produce Geographical Information for Land Planning Using Very High Resolution Images. LAP LAMBERT. Academic Publishing.
Santos, T., Lobato, K., Rocha, J., Tenedório, J.A., 2020. Modeling photovoltaic potential for bus shelters on a city-scale: a case study in Lisbon. Appl. Sci. 10, 4801. https://doi.org/10.3390/app10144801.
Singh, K., Hachem-Vermette, C., D'Almeida, R., 2023. Solar neighborhoods: the impact of urban layout on a large-scale solar strategies application. Sci. Rep. 13, 18843. https://doi.org/10.1038/s41598-023-43348-8.
Tian, A., Zünd, D., Bettencourt, L.M.A., 2021. Estimating rooftop solar potential in urban environments: a generalized approach and assessment of the galápagos islands. Front. Sustain. Cities. 3. https://doi.org/10.3389/frsc.2021.632109.
van Esch, M.M.E., Looman, R.H.J., de Bruin-Hordijk, G.J., 2012. The effects of urban and building design parameters on solar access to the urban canyon and the potential for direct passive solar heating strategies. Energy Build. 47, 189–200. https://doi.org/10.1016/j.enbuild.2011.11.042.

Vujovic, S., Haddad, B., Karaky, H., Sebaibi, N., Boutouil, M., 2021. Urban heat island: causes, consequences, and mitigation measures with emphasis on reflective and permeable pavements. CivilEng 2, 459–484. https://doi.org/10.3390/civileng2020026.

Yoshimura, Y., Kumakoshi, Y., Fan, Y., Milardo, S., Koizumi, H., Santi, P., Murillo Arias, J., Zheng, S., Ratti, C., 2022. Street pedestrianization in urban districts: economic impacts in Spanish cities. Cities 120. https://doi.org/10.1016/j.cities.2021.103468.

Zhang, J., Heng, C.K., Malone-Lee, L.C., Hii, D.J.C., Janssen, P., Leung, K.S., Tan, B.K., 2012. Evaluating environmental implications of density: a comparative case study on the relationship between density, urban block typology and sky exposure. Autom. ConStruct. 22, 90–101. https://doi.org/10.1016/j.autcon.2011.06.011.

Zhu, R., You, L., Santi, P., Wong, M.S., Ratti, C., 2019. Solar accessibility in developing cities: a case study in Kowloon East, Hong Kong. Sustain. Cities Soc. 51, 101738. https://doi.org/10.1016/j.scs.2019.101738.

Zipori, E., Cohen, M.J., 2015. Anticipating post-automobility: design policies for fostering urban mobility transitions. Int. J. Urban Sustain. Dev. 7, 147–165. https://doi.org/10.1080/19463138.2014.991737.